Ⅳ. 研究成果の刊行物・別刷

27

Confocal Microscopy for Intracellular Co-Localization of Proteins

Toshiyuki Miyashita

Abstract

Confocal laser scanning microscopy is the best method to visualize intracellular co-localization of proteins in intact cells. Because of the point scan/pinhole detection system, light contribution from the neighborhood of the scanning spot in the specimen can be eliminated, allowing high *Z*-axis resolution. Fluorescence detection by sensitive photomultiplier tubes allows the usage of filters with a narrow bandpath, resulting in minimal cross-talk (overlap) between two spectra. This is particularly important in demonstrating co-localization of proteins with multicolor labeling. Here I describe the methods outlining the detection of transiently expressed tagged proteins and the detection of endogenous proteins. Ideally, the intracellular co-localization of the two endogenous proteins should be demonstrated. However, when antibodies raised against the protein of interest are unavailable for immunofluorescence, or the available cell lines do not express the protein of interest sufficiently enough for immunofluorescence, an alternative method is to transfect cells with expression plasmids that encode tagged proteins and stain the cells with anti-tag antibodies after transient transfection. However, it should be noted that the tagging of proteins of interest or their overexpression could potentially alter the intracellular localization or the function of the target protein.

Key Words

Confocal microscopy; immunofluorescence; multicolor labeling; laser; fluorophore.

1. Introduction

Confocal laser scanning microscopy is the best method to visualize intracellular co-localization of proteins in intact cells. Confocal laser scanning microscopy offers significant advantages for viewing subcellular localization of proteins compared with conventional fluorescence microscopy.

First of all, the point scan/pinhole detection system eliminates light contribution from the neighborhood of the scanning spot in the specimen (**Fig. 1**).

From: *Methods in Molecular Biology, vol. 261: Protein–Protein Interactions: Methods and Protocols*
Edited by: H. Fu © Humana Press Inc., Totowa, NJ

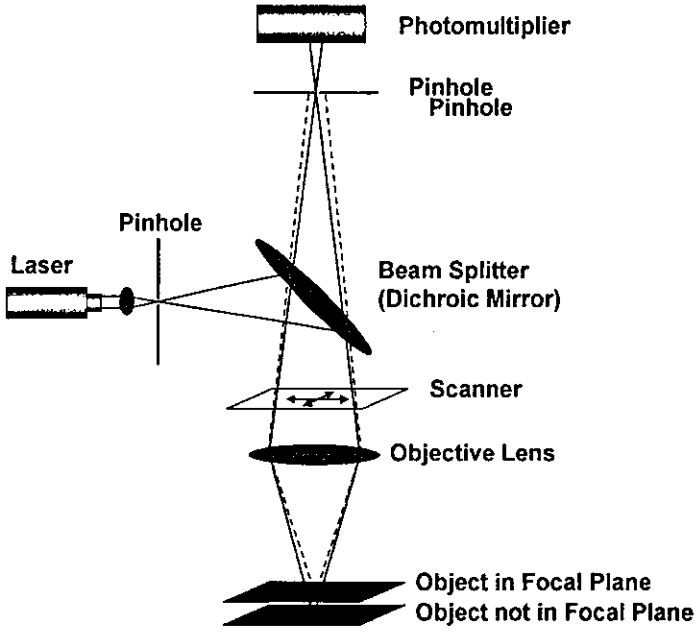

Fig. 1. Schematic diagram of the light path.

Therefore, high *Z*-axis resolution as well as *X*-*Y* image can be obtained. Fluorescence detection by sensitive photomultiplier tubes (PMT) allows the usage of filters with a narrow bandpath, resulting in minimal cross-talk (overlap) between two spectra. This is particularly important in demonstrating co-localization of proteins with multicolor labeling. In addition, digital images obtained with PMT are easy to record, modify, and transfer. Transmitted light images can be obtained by use of a transmitted light detector, but the images will not be confocal images. The transmitted light image can be used in combination with a fluorescence image to demonstrate fluorescent localization. It should kept in mind that co-localization of two proteins does not necessarily mean their physical association. Other methodologies, such as co-immunoprecipitation, should be combined to confirm the interaction.

2. Materials

1. Confocal laser scanning microscope (CLSM) (Olympus FLUOVIEW FV300 or equivalent).
2. Tissue culture equipment.
3. HeLa cells.
4. Plasmids encoding GFP-tagged or HA-tagged proteins of interest.

5. Lab-Tek II chamber slide with cover (Nalge Nunc International; Naperville, IL).
6. Effectene transfection reagent (Qiagen; Valencia, CA).
7. Phosphate-buffered saline (PBS).
8. 4% paraformaldehyde in PBS.
9. Permeabilization solution: 0.1% TritonX-100 in PBS.
10. Preblock solution: 10 m*M* Tris-HCl, pH 8.0, 150 m*M* NaCl, 0.1% Tween 20, 5% skim milk, 2% bovine serum albumin (should be filtered through a filter paper just before use).
11. Anti-HA mouse monoclonal antibody (HA.11, MMS-101R, CRP Inc.; Berkeley, CA) (*see* **Note 1**).
12. Secondary antibodies: TRITC (tetramethylrhodamine-isothiocyanate)-labeled rabbit anti-mouse immunoglobulin (R0270, Dako; Carpinteria, CA), Alexa Fluor 488-labeled goat anti-mouse immunoglobulin (A-11029, Molecular Probes; Eugene, OR), Alexa Fluor 546-labeled goat anti-rabbit immunoglobulin (A-11035, Molecular Probes).
13. Vectorshield® mounting medium (Vector Laboratories, Inc., Burlingame, CA).
14. Micro cover glass.
15. Rubber cement or nail polish.

3. Methods

The methods described below outline (1) the detection of transiently expressed tagged proteins and (2) the detection of endogenous proteins. To obtain multicolor images with optimum contrast and minimal cross-talk, appropriate combinations of fluorophores should be selected. The spectral properties of frequently used fluorophores and recommended lasers are listed in **Table 1**.

3. 1. Detection of Transiently Expressed GFP- and HA-Tagged Proteins

When antibodies raised against the protein of interest are unavailable for immunofluorescence, or the available cell lines do not express the protein of interest sufficiently enough for immunofluorescence, an alternative method is to transfect cells with expression plasmids that encode tagged proteins and stain the cells with anti-tag antibodies after transient transfection. However, it should be noted that the tagging of proteins of interest or their overexpression could potentially alter the intracellular localization or the function of the target protein. It is also mandatory to confirm the proper molecular weight of the expressed protein by Western blotting after verifying the plasmid by DNA sequencing *(1)*. To demonstrate that the protein of interest is localized in a particular organelle, a number of organelle-specific probes or vectors as well as organelle-specific monoclonal antibodies are available. To visualize mitochondria, for example, MitoTracker probes (Molecular Probes) and mitochondria localization vectors, such as pECFP-Mito (Clontech; Palo Alto, CA), can be used.

Table 1
Approximate Spectral Properties of Representative Fluorophores Used for Multicolor Labeling[a]

Fluorophore	Absorption (nm)	Emission (nm)	Laser	Notes
Group 1 (Green)				
FITC	490	512	Ar.488	Most widely used green fluorescent dye, easy to photobleach
EGFP	488	507	Ar.488	Brighter than wild-type GFP, for generating fusion proteins
Alexa Fluor 488	495	519	Ar.488	Brighter and more photostable than FITC
Group 2 (Red)				
TRITC	541	572	HeNe543 or Ar.Kr.568	Commonly used red fluorescent dye in combination with FITC
Texas Red	596	620	HeNe543 or Ar.Kr.568	Good spectral separation from FITC, slightly higher back ground staining *(2)*
Cy3	552	565	HeNe543 or Ar.Kr.568	Brighter than TRITC
Alexa Fluor 546	556	573	HeNe543 or Ar.Kr.568	Brighter than TRITC or Cy3
Propidium iodide	530	615	HeNe543 or Ar.Kr.568	For DNA/RNA staining
Group 3 (Blue)				
DAPI	345	425	UV.Ar.364	For nuclear staining
Hoechst33342	355	465	UV.Ar.364	For nuclear staining

[a] For multicolor labeling, choose one fluorophore from each group depending on the laser sources equipped in the CLSM, thus allowing up to three-color labeling.

3.1.1. Transfection

1. The day before transfection, seed HeLa cells at a density of 7×10^4 cells/well (when two-well chamber slides are used).
2. Incubate the cells at 37°C and 5% CO_2 in DMEM medium with 10% fetal bovine serum.
3. Prepare 0.5 µg of each plasmid that encodes GFP- or HA-tagged protein. The minimum DNA concentration should be 0.1 µg/µL.
4. Dilute the DNA in 60 µL of Buffer EC (Effectene transfection reagent kit). Add 6 µL of Enhancer and mix by vortexing for 1 s (*see* **Note 2**).
5. Incubate at room temperature for 2–5 min and spin down the mixture for a few seconds.
6. Add 10 µL of Effectene Transfection Reagent to the mixture. Mix by vortexing for 10 s.
7. Incubate the samples for 5–10 min at room temperature to allow complex formation.
8. During **step 7**, aspirate the medium from the slides and wash the cells once with PBS. Add 1 mL of fresh growth medium to each well.
9. Add the transfection complexes drop-wise onto the cells. Gently swirl the plates to ensure uniform distribution of the complexes.
10. Incubate the cells with the complexes at 37°C and 5% CO_2 for 24 h to allow for gene expression.

3.1.2. Immunofluorescence

1. Carefully aspirate the medium and add 0.5 mL/well of 4% paraformaldehyde in PBS drop-wise onto the cells (*see* **Note 3**).
2. To fix the cells, incubate the samples for 1 h at 4°C.
3. Carefully replace the solution with 0.5 mL/well of permeabilization solution.
4. Incubate the samples for 5 min at room temperature.
5. Carefully replace the solution with 0.5 mL/well of preblock solution and incubate the samples for 1 h at room temperature.
6. Carefully aspirate the preblock solution and add 0.5 mL/well of anti-HA mouse monoclonal antibody diluted with preblock solution at 1:200.
7. Incubate the samples for 1 h at room temperature (*see* **Note 4**).
8. Carefully aspirate the antibody solution and add 1 mL/well of PBS.
9. Incubate the samples for 10 min at room temperature. Gentle swirling facilitates washing efficiency.
10. Replace the solution with another 1 mL/well of fresh PBS and repeat **step 9**.
11. Carefully aspirate PBS and add 0.5 mL/well of TRITC-labeled rabbit anti-mouse immunoglobulin diluted with preblock solution. A 1:20 dilution is recommended.
12. Incubate the samples for 1 h at room temperature.
13. Carefully aspirate the antibody solution and wash the samples three times as described in **steps 8** and **9** (*see* **Note 5**).
14. Blot off excess PBS with a tissue, taking care not to allow the cells to dry out.

15. Place one drop of Vectorshield® over each well of cells and then place a micro cover glass over the entire well, taking care to minimize air bubbles.
16. Secure the cover glass with rubber cement or nail polish.

3.1.3. Confocal Laser Scanning Microscopy

Because the operation procedure of a CLSM depends on manufacturers and systems, it is not possible to generalize this procedure. This chapter is focused on the Olympus CLSM. The manufacturer's manual should be consulted for details.

1. Choose the correct combination of laser, barrier filters, and excitation dichroic mirrors for the dyes in use according to the manufacturer's recommendation. (For GFP/TRITC, the following combination is appropriate: laser combination: Ar488 nm + HeNe543 nm; barrier filters: BA510IF + BA530RIF for channel 1, BA565IF + BA590 for channel 2; dichroic mirror: DM488/543.)
2. Set the power switch of each unit to ON. To stabilize the laser beam output, allow the system to warm-up for at least 10 min after turning the laser power ON.
3. Start the FLUOVIEW software by double-clicking the FLUOVIEW icon on the desktop.
4. Place the specimen in an inverted position (in combination with an inverted microscope) on the microscope stage and turn the light path selector to "Binocular" section.
5. Engage the optimum cube for specimen dye by operating the cube turret and focus on the specimen initially using transmitted light and then quickly observe the cells with fluorescence.
6. When the area to be observed with confocal microscopy is determined, turn the light path selector to "Side port" position and rotate the cube turret so that no cube is engaged.
7. Choose the highest scan speed and set the zoom ratio to "X1." Set the channel to be acquired (brightness should be adjusted one channel at a time).
8. Click the "Focus" button to acquire repeated images at a high speed.
9. Focus on the cells of interest and adjust the image brightness. Parameters to be considered at this step are "PMT voltage," "Offset," and "Gain," each of which can be adjusted independently. The ND filters can also be selected using the LASER INTENSITY turret. Select the optimum ND filters according to the brightness of the specimen. A strong laser intensity, however, makes the fluorescence fade quickly.
10. When it is necessary to observe the detail of a specific area, the image of a limited area can be acquired by using the "Zoom" scale and the "Pan" buttons.
11. Once the appropriate parameters have been determined, stop repeated scanning, set a lower scan speed, and acquire the image by selecting the "Once" button (*see* **Notes 6** and **7**).
12. After the desired image has been acquired, save it to disk. It is possible to save images acquired with more than one channel at a time. The user can select the file

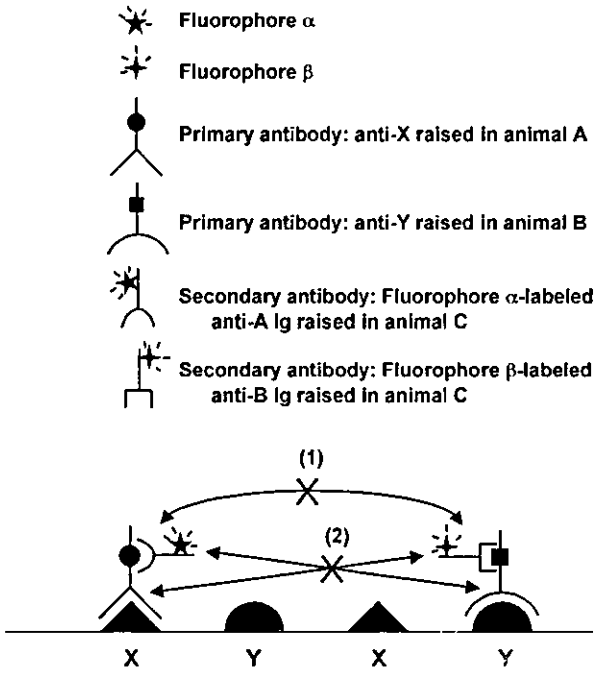

Fig. 2. Schematic diagram of multicolor detection of endogenous proteins.

types used for saving an image in a file. Fluoview Multi Tiff format is used for image analysis and processing on FLUOVIEW. Single TIF is a format for maximum portability between Macintosh and IBM PCs and programs such as Adobe Photoshop. To show the co-localization of two proteins, the merged image of the two proteins in a single view should be demonstrated as well as displaying images of the two channels side by side. For example, when the expression of a GFP-fused protein is displayed in green and that of an HA-tagged protein is shown in red, then co-localization of the two proteins is visualized in yellow in the merged image (**Figs. 3A–C**).

3. 2. Detection of Endogenous Proteins Using Labeled Secondary Antibodies

Demonstrating the intracellular co-localization of the two endogenous proteins is more convincing than showing subcellular localizations of epitope- or GFP-tagged proteins. However, the results should be obtained with highly specific primary antibodies. For example, antibodies that detect major cross-reactive bands in Western blotting are not suitable for immunofluorescence. Antibodies should also be affinity-purified prior to use to reduce background.

In addition, the cell lines used for this analysis should express the proteins of interest sufficiently enough for immunofluorescence. Two primary antibodies used in this experiment should be raised in two different species. Secondary antibodies used for simultaneous detection of more than one antigen should also be selected carefully according to the following criteria. (1) Secondary antibodies are derived from the same host species so that they do not recognize one another [**Fig. 2(1)**]. (2) They do not cross-react with other primary antibodies used in the assay system [**Fig. 2(2)**]. (3) They do not cross-react with endogenous proteins present in the cell lines under investigation. Secondary antibodies absorbed against the sera of a number of species to minimize cross-reactivity are commercially available. They are usually marked as "highly cross-absorbed" or "for multiple labeling." When cells growing in suspension are to be stained, they should be cytocentrifuged prior to the fixation using a Cytospin (Shandon; Pittsburgh, PA) or equivalent that allows low-speed centrifugal force to separate the cells on slides while maintaining cellular integrity.

1. Carefully aspirate the medium and add 0.5 mL/well of 4% paraformaldehyde in PBS dropwise onto the cells (*see* **Note 3**).
2. To fix the cells, incubate the samples for 1 h at 4°C.
3. Carefully replace the solution with 0.5 mL/well of permeabilization solution.
4. Incubate the samples for 5 min at room temperature.
5. Carefully replace the solution with 0.5 mL/well of preblock solution and incubate the samples for 1 h at room temperature.
6. Carefully aspirate the preblock solution and add 0.5 mL/well of anti-protein X mouse monoclonal antibody diluted with preblock solution. Because staining protocols vary with application, the appropriate dilution of antibody should be determined empirically.
7. Incubate the samples for 1 h at room temperature.
8. Carefully aspirate the antibody solution and add 1 mL/well of PBS.
9. Incubate the samples for 10 min at room temperature. Gentle swirling facilitates washing efficiency.
10. Replace the solution with another 1 mL/well of fresh PBS and repeat **step 9**.
11. Carefully aspirate PBS and add 0.5 mL/well of Alexa Fluor 488-labeled goat anti-mouse immunoglobulin diluted with preblock solution (1:200 or higher dilution).
12. Repeat **steps 7–10**.
13. Carefully replace the solution with 0.5 mL/well of preblock solution and incubate the samples for 1 h at room temperature. This step can be omitted depending on the antibody.
14. Carefully aspirate the preblock solution and add 0.5 mL/well of anti-protein Y rabbit polyclonal antibody diluted appropriately with preblock solution.
15. Repeat **steps 7–10**.
16. Carefully aspirate PBS and add 0.5 mL/well of Alexa Fluor 546-labeled goat anti-rabbit immunoglobulin diluted with preblock solution (1:200 or higher dilution).
17. Incubate the samples for 1 h at room temperature.

18. Carefully aspirate the antibody solution and wash the samples three times as described at **steps 8** and **9** (*see* **Note 5**).
19. Blot off excess PBS with a tissue, taking care not to allow the cells to dry out.
20. Place one drop of Vectorshield® over each well of cells and then place a micro cover glass over the entire well, taking care to minimize air bubbles.
21. Secure the cover glass with rubber cement or nail polish.

Confocal laser scanning microscopy can be performed using the same combinations of lasers, barrier filters, and dichroic mirror as described in **Subheading 3.1.3.** (channel 1 for Alexa Fluor 488, channel 2 for Alexa Fluor 546). Examples of multicolor labeling of HeLa cells are demonstrated in **Fig. 3D–I**.

4. Notes

1. Other representative anti-tag antibodies are described below. Recommended dilutions to start with are indicated in parentheses.
   a. Anti-FLAG (M2) mouse monoclonal antibody (1:100; F3165, Sigma; St. Louis, MO).
   b. Anti-His (His-probe, H-15) rabbit polyclonal antibody (1:200; sc-803, Santa Cruz; Santa Cruz, CA).
   c. Anti-c-Myc (9E10) mouse monoclonal antibody (1:100; sc-40, Santa Cruz).
2. To achieve optimal transfection efficiency for every new cell line/plasmid DNA combination, it is recommended to optimize the amounts of Effectene Reagent, DNA, and the cell number prior to transfection according to manufacturer's protocol. Other transfection reagents such as FuGene 6 (Roche) can also be used.
3. The alternative method to fix and permeabilize cells is to use methanol or acetone. The method should be selected empirically depending on the cell lines and antibodies.
4. Fluorophore-conjugated anti-tag antibodies are also available. In this case, go to **step 13**.
5. If the confocal laser scanning microscope is equipped with a UV laser, it is recommended to add 1.25 μM of Hoechst33342 (**Table 1**) to the second wash for the nuclear counterstaining. This allows observation of the location of the nucleus.
6. To improve the image quality by reduction of noise, the Kalman accumulation is recommended. It allows acquiring of images for the specified number of times while averaging the images.
7. For a double-labeled specimen, there are two alternatives to obtain the image, sequential acquisition and simultaneous acquisition. With the former image-capturing method, the image slice of each laser excitation is obtained using one PMT at a time. This scan is of advantage in acquiring an image with a lower cross-talk between two wavelengths. In contrast, with a simultaneous scan, images without a time lag between two wavelengths are obtained.

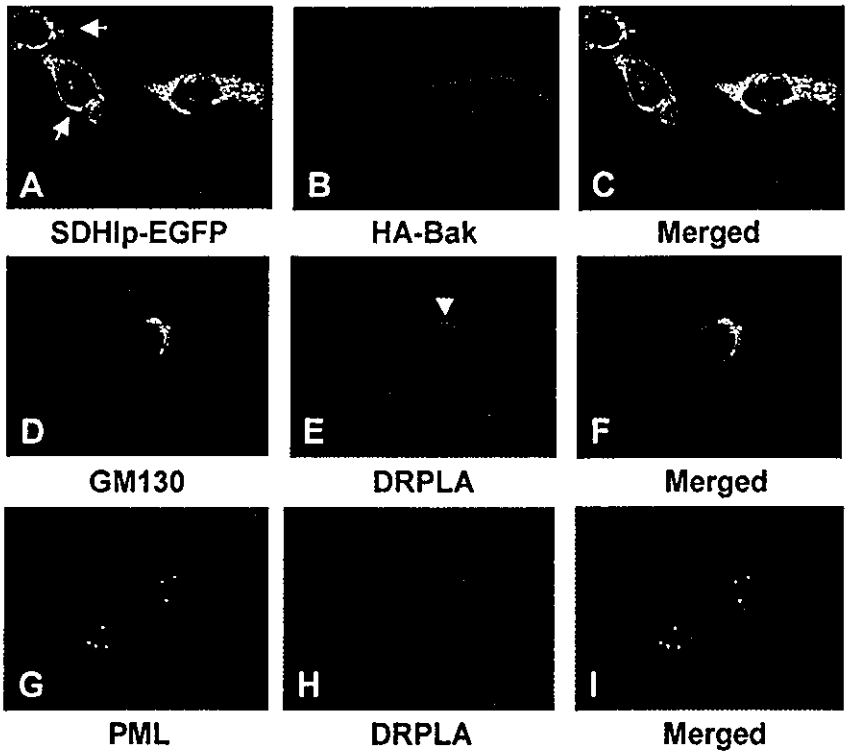

Fig. 3. Multicolor labeling of HeLa cells. **(A–C)** HeLa cells were transfected with pSDHIp-EGFP and pHA-Bak that encode the EGFP-tagged iron sulfur subunit of human succinate dehydrogenase *(3)* and HA-tagged proapoptotic Bcl-2 family member, Bak *(4,5)*, respectively. At 24 h after transfection, cells were stained with anti-HA antibody followed by TRITC-labeled secondary antibody. Panels **A** and **B** show the subcellular localizations of SDHIp and Bak, respectively. Merged pictures are shown in panel **C**. SDHIp is a mitochondrial protein and Bak is shown to co-localize with SDHIp. Arrows indicate cells transfected with only pSDHIp-EGFP. **(D–F)** HeLa cells were incubated with mouse anti-GM130 monoclonal antibody (BD transduction Laboratories, San Diego, CA) and rabbit anti-DRPLA antibody *(6)*. The primary antibodies were detected by secondary antibodies conjugated to Alexa Fluor 488 or 546. DRPLA protein, a product of the gene responsible for a genetic neurodegenerative disease, dentatorubral-pallidoluysian atrophy (DRPLA) *(7)*, is localized in the nucleus *(8)*. However, a closer observation reveals that it is also localized in the juxtanuclear region (arrowhead) where it co-localizes with GM130 **(F)**, which is a *cis*-Golgi network marker *(9)*. **(G–I)** HeLa cells were treated similarly as in **D–F** except that anti-PML mouse monoclonal antibody (Santa Cruz) was used as one of the primary antibodies. The promyelocytic leukemia (PML) protein is a major component of nuclear dot-like structures known as PML nuclear bodies (NBs) or PML oncogenic domain (POD) *(10,11)* **(G)**. These panels show that the nuclear DRPLA protein is not recruited to NBs or POD.

Acknowledgments

I thank Yuko Ohtsuka and Mami U for their technical assistance. I am also grateful to Drs. Yoshiaki Shikama and Yuko Okamura-Oho for their valuable discussions.

References

1. Sambrook, J. and Russell, D. W. (2001) *Molecular Cloning, A Laboratory Manual*, 3rd Ed. Cold Spring Harbor Laboratory Press, Cold Spring Harbor, New York, NY.
2. Wessendorf, M. W. and Brelje, T. C. (1992) Which fluorophore is brightest? A comparison of the staining obtained using fluorescein, tetramethylrhodamine, lissamine rhodamine, Texas red, and cyanine 3.18. *Histochemistry* **98,** 81–85.
3. Kita, K., Oya, H., Gennis, R. B., Ackrell, B. C., and Kasahara, M. (1990) Human complex II (succinate-ubiquinone oxidoreductase): cDNA cloning of iron sulfur (Ip) subunit of liver mitochondria. *Biochem. Biophys. Res. Commun.* **166,** 101–108.
4. Chittenden, T., Harrington, E. A., O'Connor, R., et al. (1995) Induction of apoptosis by the Bcl-2 homologue Bak. *Nature* **374,** 733–736.
5. Kiefer, M. C., Brauer, M. J., Powers, V. C., et al. (1995) Modulation of apoptosis by the widely distributed Bcl-2 homologue Bak. *Nature* **374,** 736–739.
6. Miyashita, T., Okamura-Oho, Y., Mito, Y., Nagafuchi, S., and Yamada, M. (1997) Dentatorubral pallidoluysian atrophy (DRPLA) protein is cleaved by caspase-3 during apoptosis. *J. Biol. Chem.* **272,** 29,238–29,242.
7. Nagafuchi, S., Yanagisawa, H., Ohsaki, E., et al. (1994) Structure and expression of the gene responsible for the triplet repeat disorder, dentatorubral and pallidoluysian atrophy (DRPLA). *Nat. Genet.* **8,** 177–182.
8. Miyashita, T., Nagao, K., Ohmi, K., Yanagisawa, H., Okamura-Oho, Y., and Yamada, M. (1998) Intracellular aggregate formation of dantatorubral-pallidoluysian atrophy (DRPLA) protein with the extended polyglutamine. *Biochem. Biophys. Res. Commun.* **249,** 96–102.
9. Nakamura, N., Rabouille, C., Watson, R., et al. (1995) Characterization of a cis-Golgi matrix protein, GM130. *J. Cell Biol.* **131,** 1715–1726.
10. Dyck, J. A., Maul, G. G., Miller, W. H. J., Chen, J. D., Kakizuka, A., and Evans, R. M. (1994) A novel macromolecular structure is a target of the promyelocyte-retinoic acid receptor oncoprotein. *Cell* **76,** 333–343.
11. Weis, K., Rambaud, S., Lavau, C., et al. (1994) Retinoic acid regulates aberrant nuclear localization of PML-RAR alpha in acute promyelocytic leukemia cells. *Cell* **76,** 345–356.

Liver International 2004: 24: 259–267
Printed in Denmark. All rights reserved

Liver International
DOI: 10.1111/j.1478-3231.2004.0909.x

Original Article

Hepatitis C virus infection in human liver tissue engrafted in mice with an infectious molecular clone

Maeda N, Watanabe M, Okamoto S, Kanai T, Yamada T, Hata J, Hozumi N, Katsume A, Nuriya H, Sandhu J, Ishii H, Kohara M, Hibi T. Hepatitis C virus infection in human liver tissue engrafted in mice with an infectious molecular clone.
Liver International 2004: 24: 259–267. © Blackwell Munksgaard 2004

Abstract: *Background/aims:* Recent advances in molecular cloning of hepatitis C virus (HCV) have enabled us to apply some available HCV molecular clones to experimental studies. However, these investigations have been restricted to chimpanzee models or 'isolated hepatocytes' from tree shrews. In this study, we engrafted 'human liver tissue' into immunodeficient mice and investigated HCV infection using an infectious molecular clone. *Methods:* Human liver tissues from normal (non-HCV-infected) liver were transplanted into non-obese diabetic/severe combined immunodeficiency (NOD/SCID) mice. We then inoculated the mice with sera from HCV-infected patients or an infectious HCV molecular clone. HCV RNA was assessed using nested reverse-transcription polymerase chain reaction (PCR), real-time detection PCR and *in situ* PCR. *Results:* Without any growth support, normal human liver tissues survived in NOD/SCID mice while maintaining the original viable hepatic architecture. HCV RNA was detected in the mice serum until the fourth week after the inoculation. *In situ* PCR and immunohistochemistry clearly demonstrated positive signals for HCV in the cytoplasm of infected hepatocytes, while the engrafted human liver tissues showed no apparent morphological changes indicative of infection. *Conclusion:* Engraftment of human liver tissues into NOD/SCID mice and infection with HCV molecular clones could offer a reverse genetic strategy for HCV infection.

Norio Maeda[1], Mamoru Watanabe[2], Susumu Okamoto[1], Takanori Kanai[2], Taketo Yamada[3], Jun-ichi Hata[3], Nobumichi Hozumi[4], Asao Katsume[5], Hideko Nuriya[5], Jasbir Sandhu[6], Hiromasa Ishii[1], Michinori Kohara[5] and Toshifumi Hibi[1]

[1]Department of Internal Medicine, School of Medicine, Keio University, Tokyo, Japan, [2]Department of Gastroenterology and Hepatology, Graduate School, Tokyo Medical and Dental University, Tokyo, Japan, [3]Department of Pathology, School of Medicine, Keio University, Tokyo, Japan, [4]Research Institute for Biological Sciences, Science University of Tokyo, Tokyo, Japan, [5]Department of Microbiology and Cell Biology, Tokyo Metropolitan Institute of Medical Science, Tokyo, Japan, [6]Department of Surgery, Faculty of Medicine, University of Toronto, Toronto, Canada

Key words: hepatitis C virus – human liver tissue – infectious molecular clone – *in situ* PCR – NOD/SCID mouse

Toshifumi Hibi, Department of Internal Medicine, Keio University School of Medicine, 35 Shinanomachi, Shinjuku-ku, Tokyo 160-8582, Japan.
Tel: 81-3-3357-6286
Fax: 81-3-3357-6156
e-mail: thibi@sc.itc.keio.ac.jp

Received 18 July 2003,
accepted 4 February 2004

Hepatitis C virus (HCV) is the major causative agent of posttransfusion-associated hepatitis and of most sporadic non-A, non-B hepatitis (1). Persistent HCV infection often progresses to chronic hepatitis, liver cirrhosis and hepatocellular carcinoma (2). Biological evaluation of HCV has been hampered because of the lack of small animal models for HCV infection and efficient *in vitro* culture systems for the virus.

Recent advances in molecular cloning of HCV genome have allowed the development of infectious molecular clones and they have been applied extensively in experimental investigation (3–6). Investigation of HCV infection using a well-characterized infectious molecular clone as the inoculum will provide valuable information to us about the underlying mechanisms of HCV infection. However, previous studies on *in vivo* infection of HCV molecular clones were restricted to inoculation into chimpanzees (3, 5, 6).

Only a few experimental studies on HCV infection using small animal models have been reported (7, 8). Recently it was reported that HCV could infect and replicate in an immunodeficient transgenic mouse model bearing chimeric 'isolated human hepatocytes' (9, 10), and this

indicated that a mouse model for HCV infection was feasible. However, it has been postulated that HCV itself is not directly cytopathic for hepatocytes (11) and that the immune response mediated by hepatocytes, lymphocytes, macrophages, Kupffer cells and the extracellular matrix play essential roles in the pathogenesis of HCV hepatitis (12–14). Therefore, an *in vivo* experimental study using small animals engrafted with human 'liver tissue' would be of advantage to clarify the mechanisms of HCV infection.

The SCID-hu system (15) is a well-known animal model for the introduction of human tissues into SCID mice and has been applied extensively to study the behavior of some infectious viruses (16, 17). Non-obese diabetic/severe combined immunodeficiency (NOD/SCID) mice are a strain recently established by crossing SCID mice with NOD mice that show characteristic immunologic dysfunctions (18), which enable better engraftment of several human tissues than SCID mice, for the original architecture of the grafts is well preserved (19, 20). Therefore, the human liver tissues engrafted in NOD/SCID mice are expected to be suitable to investigate HCV infection.

In this study, we transplanted normal (non-HCV-infected) human liver tissue blocks into NOD/SCID mice and investigated HCV infection with an infectious molecular clone as well as the conventional serum inoculum.

Materials and methods

Mice

NOD/SCID mice were kindly provided by the Jackson Laboratory (Bar Harbor, ME). The animals were used at 6–10 weeks of age, and were fed sterile food under SPF conditions. The Animal Care Committee of the Keio University Hospital approved the experiments protocol.

Liver tissue

Non-HCV-infected human liver tissues were obtained at the partial hepatectomy from patients with liver tumors. They were examined by two pathologists to confirm non-cirrhotic non-tumorous changes. HCV-infected human liver tissues were obtained at the surgical resection of hepatoma from patients with chronic hepatitis. Tissue specimens were immediately stored at 4 °C in RPMI medium supplemented with 10% FCS until transplantation. The protocols of experiments in humans were approved by the Keio University Hospital Committee on Human Subjects, and written informed consent was obtained from all the patients.

Transplantation procedures

Non-HCV-infected and HCV-infected human liver tissues were cut into small fragments of 3–4 mm^3 with microsurgical knives, and the fragments were transplanted under the kidney capsule of NOD/SCID mice under anesthesia with Nembutal (Fig. 1). In preliminary experiments, we engrafted human liver tissues in the subcutis, liver and peritoneum to find a suitable anatomic site for engraftment.

In vivo infection with sera from HCV-infected patients and infectious HCV molecular clone

Human serum containing a high titer of HCV RNA (9.3×10^6–1.5×10^8 copies/ml) was obtained from five patients with chronic active hepatitis. All patients tested seropositive for

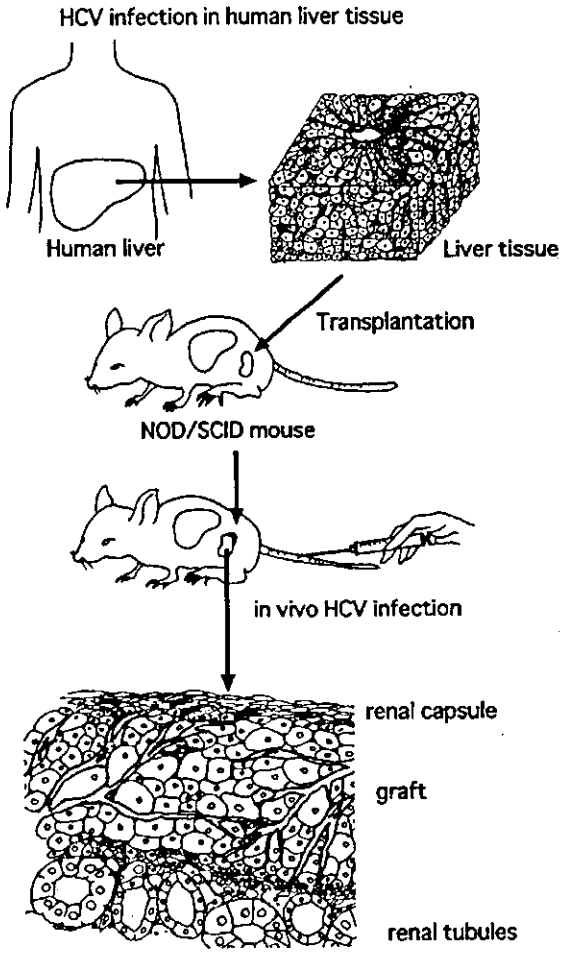

Fig. 1. Hepatitis C virus (HCV) infection in human liver tissue. Schematic representation of the procedure employed to induce *in vivo* HCV infection in human liver tissue.

HCV antibodies according to a second-generation ELISA and seronegative for hepatitis B virus, and had 1b or 2a genotype of HCV. The individual serum samples were divided into small aliquots and kept at −80 °C separately. The infectious cDNA clone (genotype 1b) used for this study was prepared as previously described (21) with some modifications (Kohara M, et al., unpublished data). Two days after liver tissue transplantation, each group of two mice was intravenously inoculated with 100 µl of the individual patient's serum and another group of five mice with 100 µl of culture medium containing 1×10^7 copies of the HCV genome. We examined liver tissue from five patients.

Histological examination and immunohistochemical analysis

Transplanted grafts of human liver tissues were formalin fixed, paraffin embedded and assessed by hematoxylin–eosin (H&E) staining and immunohistochemistry using conventional ABC method at various points after transplantation, between the first and the 12th week. The following antibodies related to human liver were used: albumin, α-1-antitrypsin, cytokeratin 8, cytokeratin 19, CD34, CD45RO and CD20 (Dako, Japan, Kyoto). A monoclonal antibody specific for non-structural protein 3 of HCV (clone; MMM33) was used with indirect alkaline phosphatase-labeled antibody method according to the instructions provided by the manufacturer (Novocastra, Newcastle upon Tyne, UK).

Nested reverse-transcription polymerase chain reaction (nested RT-PCR) analysis for HCV RNA

Serum samples were collected weekly after liver tissue transplantation and were analyzed for HCV RNA by nested RT-PCR. RNA was extracted using the SepaGene RV-R RNA extraction system (Sanko Junyaku, Tokyo, Japan), then it was dissolved in RNase-free water. cDNA for the positive-strand RNA was synthesized using 50 ng of the antisense primer ASI in a reaction mixture containing 1 × Taq polymerase buffer, 0.5 mM dNTP, 20 U of RNAsin (Promega, Madison, WI), 10 mM dithiothreitol and 30 U of avian myeloblastosis virus reverse transcriptase (Life Sciences, Bethesda, MD) for 60 min at 42 °C. The initial reaction mixture included Taq polymerase buffer, 2 mM dNTP, 1.5 mM $MgCl_2$, 20 ng of the other primer SI and 2.5 U of Taq polymerase. The PCR consisted of 35 cycles, consisting of incubation at 94 °C for 1.5 min, at 55 °C for 1.5 min and at 72 °C for 3 min. The second PCR was done using the first PCR reaction mixture and the nested set of primers SII and ASII. The primers were from the 5′ untranslated region: SI (nts 7–26), 5′-ACTCCACCATAGATCACTCC-3′; ASI (nts 248–229), 5′-AACACTACTCGGCTAGCAGT-3′; SII (nts 46–65), 5′-TTCACGCAGAAAGCGTCTAG-3′; ASII (nts 190–171), 5′-GTTGATCCAAGAAAGGACCC-3′.

Real-time detection (RTD)-PCR

Quantitative RTD-PCR assay based on the TaqMan Chemistry system (PerkinElmer, Foster City, CA) was performed using the ABI Prism 7700 sequence detector (PerkinElmer) as previously described (22).

In situ PCR analysis for HCV RNA

In situ RT-PCR of HCV RNA was performed as previously described with some modifications (23, 24). OCT-embedded liver tissues were sectioned at a thickness of 10 µm and placed on silane-coated glass slides, fixed overnight in 10% formaldehyde at room temperature, and then treated with 0.01 µg/ml proteinase K at 37 °C for 30 min. For the reverse transcription procedure, Moloney Murine Leukemia Virus reverse transcriptase (GIBCO BRL, Grand Island, NY) was used. The sections were incubated for 60 min at 42 °C under a coverslip in the following reaction mixture: 10 mM Tris HCl, 50 mM KCl, 5.0 mM $MgCl_2$, 1 mM dNTP, 2 U/µl ribonuclease inhibitor (Takara, Shiga, Japan), 1 µM antisense primer for HCV, 10 mM DTT and 10 U/µl reverse transcriptase. In each experiment, sections that were omitted in the RT step were processed for *in situ* PCR as controls. We also examined the endogenous mouse liver from the HCV-inoculated mice. *In situ* PCR reaction was carried out using an In Situ PCR System 1000 (PerkinElmer) in the following reaction mixture: 10 mM Tris HCl, 50 mM KCl, 1.5 mM $MgCl_2$, 0.8 µM HCV primers. The primers were from the 5′ untranslated region, sense (nts 129–147): 5′-CCGGGAGAGCCATAGTGGT-3′, and antisense (nts 272–290): 3′-GCTTTCCGGAACACCATGA-5′), 197 µM dNTP and 10 U Taq gold polymerase. After denaturation, 15–30 cycles of amplification, each of them consisting of incubation at 95 °C for 30 s and at 60 °C for 2 min, were performed. The samples were then fixed in 4% paraformaldehyde for 10 min. The PCR products were then detected by *in situ* hybridization using a digoxigenin-labeled oligonucleotide probe as follows: 5′(DIG)-ATTTGGGCTGTGCCCCCGCGAGACTGCTAGCCGAGTAGTGTTGGGT-3′ (DIG)n (nts 225–269).

Results

Engraftment of normal (non-HCV-infected) and HCV-infected liver tissues in NOD/SCID mice

Approximately 90% of normal and HCV-infected human liver tissues transplanted under the kidney capsule survived throughout this experimental study. Histological examination showed that 71 (60%) of 118 transplanted grafts of normal human liver tissue were viable during 4 weeks after transplantation (Figs 2–4 and Table 1), but regression of hepatocytes, fibrous and granulomatous changes were predominant after that. In other transplanted sites, namely, the subcutis, liver and peritoneum, the original hepatic architecture of the graft was replaced by fibrous and granulomatous tissues and disappeared on the second week. Twelve (63%) of 19 transplanted grafts of HCV-infected human liver tissue were viable for 4 weeks. HCV RNA appeared in mouse serum on the first week after engraftment and it was detected until fourth week by nested RT-PCR, and the viral titer ranged from 410 to 760 copies/ml by RTD-PCR. Immunohistochemistry using antibodies related to human liver tissue clearly demonstrated the grafts were of human origin (Table 2). Positive staining for human hepatocyte markers, albumin and α-1-antitrypsin suggested that the engrafted liver tissue was viable and functional. Furthermore, engrafted liver tissues were stained positively for cytokeratin 8, cytokeratin 19, CD45RO (UCHL-1), CD20 (L26) and CD34 (Fig. 5). These immunohistochemical results indicated that the microenvironment of human liver tissue was maintained throughout the experiments.

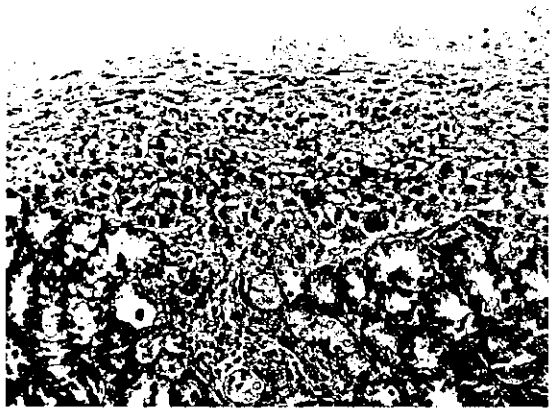

Fig. 2. Engraftment of normal human liver tissue in non-obese diabetic/severe combined immunodeficiency mouse. Microphotograph of the graft (hematoxylin–eosin staining), harvested on the second week after transplantation. Transplanted human liver tissue adjacent to the renal tubules was covered by a fibrovascular capsule (original magnification ×225).

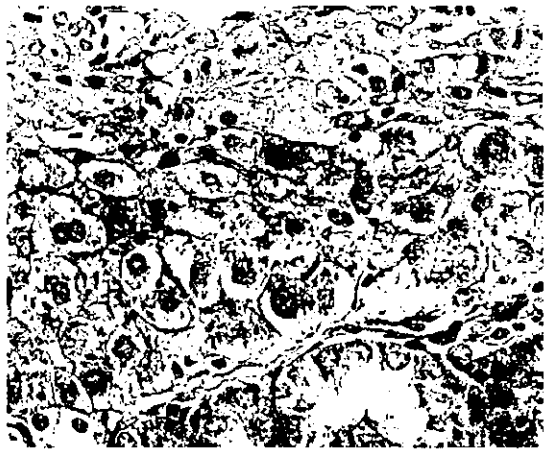

Fig. 3. High-magnification microphotograph of Fig. 2. The architecture of human liver tissue was well preserved without apparent signs of injury caused by transplantation (original magnification ×600).

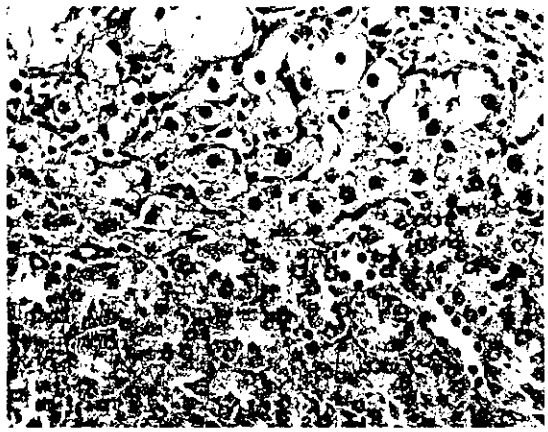

Fig. 4. Engraftment of hepatitis C virus-infected human liver tissue in non-obese diabetic/severe combined immunodeficiency mouse. Microphotograph of the graft (hematoxylin–eosin staining). Well-preserved viable hepatocytes, Kupffer cells and capillaries were observed. Hepatocytes appeared focally swollen and infiltrating small round cells were observed in the entire liver tissue. These findings were compatible with the features of chronic hepatitis (original magnification ×400).

In vivo infection with sera from HCV-infected patients and infectious HCV molecular clone

The positive-strand HCV RNA was detected by nested RT-PCR in the mice serum obtained during the first to the fourth week when inoculated with a patient's serum of 1b genotype (Table 3). The viral titer of the mouse serum inoculated with HCV-infected human serum was quantified from 450 to 910 copies/ml by RTD-PCR, and the viremia lasted 4 weeks as long as the liver tissue grafts were viable. Immunohistochemical examination using a monoclonal antibody specific for NS3 of HCV demonstrated the positive signal in the cytoplasm of the infected hepatocytes (Fig. 9).

Table 1. Engraftment of normal (non-HCV-infected) and HCV-infected human liver tissues in NOD/SCID mice

Weeks after transplantation	No. of mice successfully engrafted/total	
	Normal (non-HCV-infected)	HCV-infected
1–4	71/118	12/19
5–	1/10	2/10
Total	72/128	14/29

HCV, hepatitis C virus; NOD/SCID, non-obese diabetic/severe combined immunodeficiency.

Table 2. Immunohistochemistry of engrafted human liver tissues in NOD/SCID mice

	Human liver tissue	
	Normal (non-HCV-infected)	HCV-infected
Albumin	++	++
α-1-antitrypsin	+	+
Cytokeratin 8	++	++
Cytokeratin 19	+	+
CD34	+	+
CD45RO (UCHL-1)	+	++
CD20 (L26)	+	+

++, +, positive. Engrafted human liver tissues were examined on the second week after transplantation. NOD/SCID, non-obese diabetic/severe combined immunodeficiency; HCV, hepatitis C virus.

Table 3. *In vivo* infection with sera from HCV-infected patients

Source of serum	Genotype	Viral titer by RTD-PCR (copies/ml)	HCV RNA in mice sera by nested RT-PCR
Pt. A	1b	1.5×10^8	Positive
Pt. B	1b	5.3×10^7	ND
Pt. C	1b	9.6×10^7	ND
Pt. D	1b	7.5×10^7	ND
Pt. E	2a	9.3×10^6	ND

ND, not detected; HCV, hepatitis C virus; RT-PCR, reverse-transcription polymerase chain reaction; RTD, real-time detection.

Table 4. *In vivo* infection with infectious HCV molecular clone

Source of liver tissue	Primary tumor of liver metatasis	HCV RNA mice sera by nested RT-PCR
Pt. F	Rectal ca.	Positive
Pt. G	Rectal ca.	Positive
Pt. H	Colon ca.	Positive
Pt. I	Colon ca.	Positive
Pt. J	Colon ca.	ND

ND, not detected; ca., carcinoma; HCV, hepatitis C virus; RT-PCR, reverse-transcription polymerase chain reaction.

We then inoculated the mice with the culture medium containing the infectious HCV molecular clone. The positive-strand HCV RNA was detected by nested RT-PCR in the mice sera from four out of five individual liver tissue transplantation (Table 4). In representative data, it was detected in four out of five mice at the first week (Fig. 6), while the viral titer of the mouse serum was close to the detection limit of 440 copies/ml by RTD-PCR. However, histological examination with H&E staining at the first week after inoculation demonstrated viable hepatocytes without any apparent morphological changes indicative of HCV infection and showed no different features from normal hepatocytes (Fig. 7). To confirm whether HCV had infected the grafts, we investigated the engrafted liver tissue sections using *in situ* PCR. In seroposive cases,

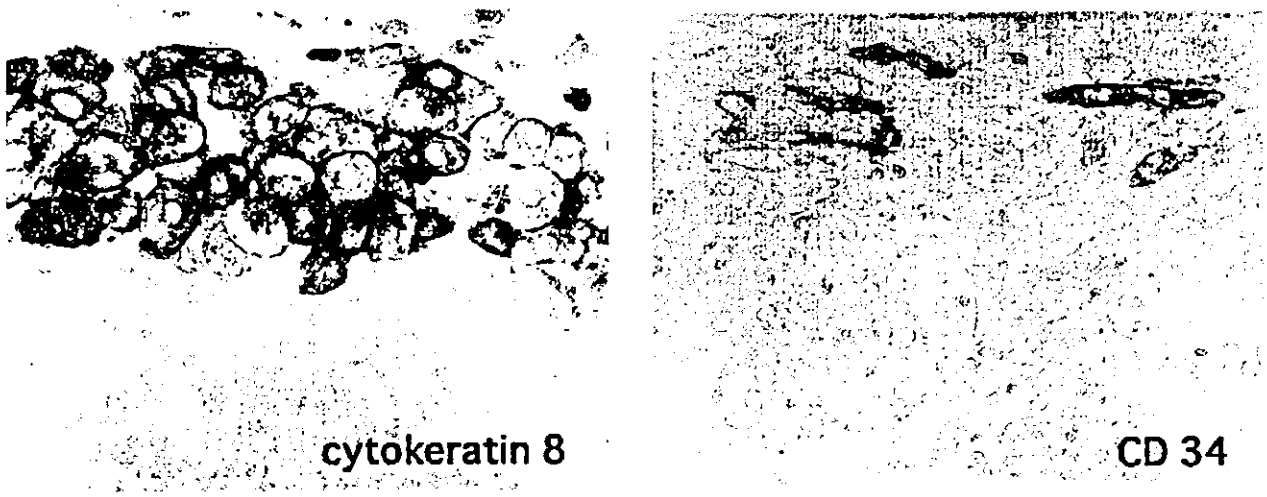

Fig. 5. Immunohistochemical staining with cytokeratin 8 and with CD34. The grafts derived from human liver tissue were easily recognized with cytokeratin 8 staining rather than with conventional hematoxylin–eosin staining (left panel: original magnification × 600). Human-derived vascular endothelial cells were demonstrated on the luminal surface of the capillaries that stained positive for CD34 (right panel: original magnification × 600).

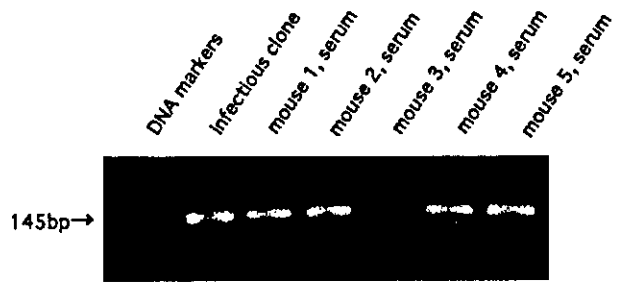

Fig. 6. Experimental hepatitis C virus (HCV) infection of engrafted normal human liver tissue with an infectious molecular clone. The positive-strand HCV RNA was detected by nested reverse-transcription polymerase chain reaction in four of five mice serum in a representative case (Pt. F) at 1 week after the inoculation. DNA markers, molecular weight markers: infectious clone, positive control; mouse 1–5 represents each mouse serum.

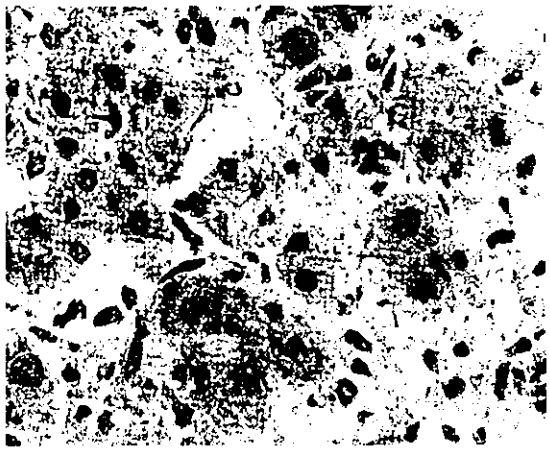

Fig. 7. Experimental hepatitis C virus (HCV) infection of engrafted normal human liver tissue with an infectious molecular clone. Microphotograph of the graft examined in the experiment described in Fig. 6, which was harvested 1 week after the inoculation (frozen section, hematoxylin–eosin staining). Viable hepatocytes, without any apparent morphological change indicative of HCV infection, were observed (original magnification ×600).

signals for positive-strand HCV RNA were focally detected by *in situ* PCR in the cytoplasm of the engrafted hepatocytes (Fig. 8a). Approximately 10–20% of hepatocytes were estimated to be infected with HCV as assessed by *in situ* PCR. Positive signals were detected neither on sections that were omitted in the RT step (Fig. 8b) nor on the endogenous mouse liver from the HCV-inoculated mice (Fig. 8c).

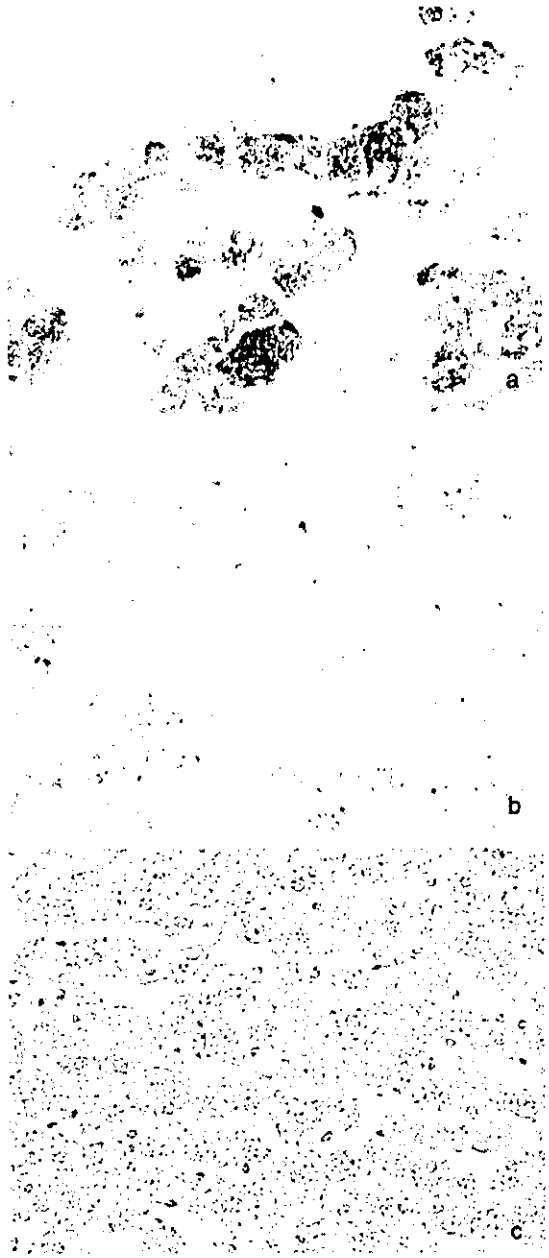

Fig. 8. Experimental hepatitis C virus (HCV) infection of engrafted normal human liver tissue with an infectious molecular clone. *In situ* polymerase chain reaction (PCR) was done using the same specimen examined in the experiment described in Fig. 7. *In situ* PCR demonstrated the positive-strand HCV RNA in the engrafted human liver tissue. (a) Positive signals were observed in the cytoplasm of the engrafted hepatocytes in cluster, while no signals were detected either on specificity control without RT step (b) or on the endogenous mouse liver tissue (c) (original magnification × 600 (a) and (b); ×225 (c)).

Discussion

We clearly demonstrated HCV infection in human liver tissue graft with an infectious HCV molecular clone as well as with serum from HCV-infected patients by immunohistochemistry and *in situ* PCR. The infectious clone seems to be a useful inoculum that is substituted for conventional inoculum of the serum, and it also makes it possible to employ a reverse genetic approach to investigate the underlying mechanisms of HCV infection.

In this study, non-HCV-infected normal liver tissues as well as HCV-infected liver tissues were

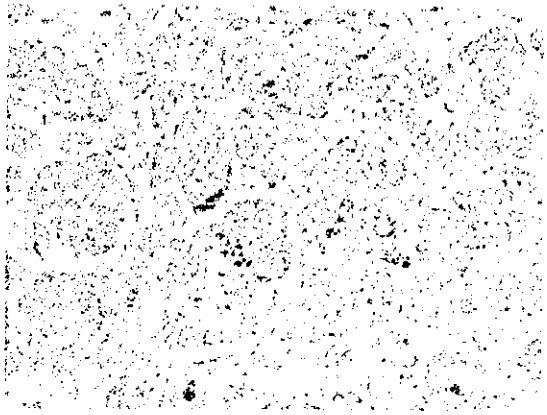

Fig. 9. Experimental hepatitis C virus (HCV) infection of engrafted normal human liver tissue with the HCV-infected patient's serum at 3 weeks after the inoculation. Immunohistochemical staining with a monoclonal antibody specific for non-structural protein 3 of HCV demonstrated the granular signal in the cytoplasm of some infected hepatocytes (indirect alkaline phosphatase-labeled antibody method; original magnification × 600).

engrafted into NOD/SCID mice. Histological and immunohistochemical examination demonstrated that the microenvironment of the human liver tissue, including hepatocytes, bile ducts, Kupffer cells and microvessels was well preserved in the graft. In NOD/SCID mice, the DNA repair gene defect of SCID mice that severely impairs B- and T-cell development combines with the reduced natural killer cell activity, absence of complement activity, and defective macrophage function of NOD mice (18). These unique immunologic characteristics allow the implanted 'human tissues' to maintain their function as well as the original architecture (19). This study revealed that the space under the kidney capsule was the most suitable site for the implantation of human liver tissue and we speculated that the space under the kidney capsule was a favorable site with respect to blood supply, rather than an 'immune-privileged site', which is a current topic for Fas ligand expression to induce apoptosis of infiltrated lymphocytes and suppress inflammatory immune response, thereby reducing allograft rejection (25, 26). In fact, we identified a fibrovascular capsule surrounding the engrafted human liver tissue. Moreover, immunohistochemical examination of the engrafted liver tissue revealed it was viable and functional without obvious signs of mechanical injury caused by transplantation procedures. Still, the typical hepatic architecture of the graft gradually disappeared with time and was replaced by fibrous and granulomatous tissue after 1 month. These phenomena might have been due, at least in part, to the absence of essential growth factors, such as human hepatocyte growth factor (27, 28), vascular endothelial growth factor (29) and IL-6 (30), as well as to the lack of liver-specific portal circulation (31) and bile clearance that probably resulted in hepatic tissue ischemia and cholestasis. Thus, the engraftment of human liver tissues into NOD/SCID mice may become a simple animal model requiring no growth support (32, 33).

Previous *in vivo* HCV infection studies were done in chimpanzees using infectious patients' sera (34). HCV, like other RNA viruses, mutates rapidly, leading to the simultaneous coexistence of heterogeneous pools in the same individual serum (quasispecies) (35). In addition, it was reported that HCV infection induced a neutralizing antibody response in experimental studies (36). For these reasons, the investigation of HCV infection using a well-characterized infectious molecular clone is suitable to provide valuable information to us with respect to the pathogenesis of HCV infection. The establishment of testing system for molecular clones is a crucial problem toward the application of the reverse genetic approach, however, it has been restricted to the chimpanzee model (3, 5, 6) or 'isolated hepatocytes' (9, 10, 37). This experimental strategy using 'human liver tissue' and the well-characterized molecular clones will enable us to pursue an *in vivo* functional analysis (38) in the early phase of HCV infection.

The viral titer of mouse serum quantified by RTD-PCR was very low, this might have been due to the low number of infected cells in the early stage of infection and, in part, to a high rate of HCV clearance at approximately 2–3 h from the serum (39). On the other hand, the detection of HCV RNA in serum using strand-specific nested RT-PCR should be considered with caution because of extensive artifactual detection of the negative-strand RNA, due to self-priming and mispriming events (40). In fact, our preliminary examination for the negative-strand RNA was not convincing for viral replication (data not shown). Therefore, we examined the positive-strand HCV RNA by nested RT-PCR to assess the presence of HCV in the serum as a supporting evidence for viral infection.

In situ detection of the HCV genome and gene products in liver tissue is a direct evidence of HCV infection and we demonstrated positive signals in the cytoplasm of infected hepatocytes by *in situ* PCR after inoculation of an infectious molecular clone. It is important to identify not only cellular tropism but also the subcellular site of viral replication, and our results were concordant with the previous reports (41). In this study, positive signals were focally detected in the engrafted hepatocytes. One week after the inoculation,

approximately only 10–20% of hepatocytes were estimated as infected by *in situ* PCR. Taken together, we performed *in situ* PCR to demonstrate HCV RNA in the early phase of infection. Another interesting fact was that the histological examination revealed no apparent morphological changes indicative of HCV infection and showed features very similar to those of non-infected hepatocytes in tissue with the original hepatic architecture. It is unclear whether HCV has direct cytopathic effects (11, 42) and our results also offered a clue to this problem.

Thus, we could clearly show that an HCV molecular clone could infect the grafts of human liver tissue as well as the patients' serum. This experimental study using human liver tissues employs a simple engraftment technique without any growth support and may offer the possibility of a strategy to assess the function of molecular clones. Further modifications using various infectious HCV molecular clones will allow a reverse genetic approach for the investigation of HCV infection, replication and the pathogenesis of liver tissue injury caused by HCV.

Acknowledgements

We thank Drs. Daniel K. Podolsky, Raymond T. Chung, Hidekazu Tsukamoto and Michael M.C. Lai for critical comments and advice, as well as Drs. Yoshio Mizuno, Hidetsugu Saito and Robert Y. Osamura for encouraging us to prepare this paper. This work was supported in part by grants-in-aid from the Japanese Ministry of Education, Culture and Science, from the Keio University Medical Science Fund and from the Tsumura Institute for Oriental Medicine, School of Medicine, Keio University, Tokyo, Japan.

References

1. Alter H J, Purcell R H, Shih J W, et al. Detection of antibody to hepatitis C virus in prospectively followed transfusion recipients with acute and chronic non-A, non-B hepatitis. N Engl J Med 1989; 321: 1494–500.
2. Saito I, Miyamura T, Ohbayashi A, et al. Hepatitis C virus infection is associated with the development of hepatocellular carcinoma. Proc Natl Acad Sci USA 1990; 87: 6547–9.
3. Kolykhalov A A, Agapov E V, Blight K J, et al. Transmission of hepatitis C by intrahepatic inoculation with transcribed RNA. Science 1997; 277: 570–4.
4. Blight K J, Kolykhalov A A, Rice C M. Efficient initiation of HCV RNA replication in cell culture. Science 2000; 290: 1972–4.
5. Yanagi M, Purcell R H, Emerson S U, et al. Transcripts from a single full-length cDNA clone of hepatitis C virus are infectious when directly transfected into the liver of a chimpanzee. Proc Natl Acad Sci USA 1997; 94: 8738–43.
6. Hong Z, Beaudet-Miller M, Lanford R E, et al. Generation of transmissible hepatitis C virions from a molecular clone in chimpanzees. Virology 1999; 256: 36–44.
7. Galun E, Burakova T, Ketzinel M, et al. Hepatitis C virus viremia in SCID → BNX mouse chimera. J Infect Dis 1995; 172: 25–30.
8. Xie Z C, Riezu-Boj J I, Lasarte J J, et al. Transmission of hepatitis C virus infection to tree shrews. Virology 1998; 244: 513–20.
9. Mercer D F, Schiller D E, Elliott J F, et al. Hepatitis C virus replication in mice with chimeric human livers. Nat Med 2001; 7: 927–33.
10. Hsu E C, Hsi B, Hirota-Tsuchihara M, Ruland J, et al. Modified apoptotic molecule (BID) reduces hepatitis C virus infection in mice with chimeric human livers. Nat Biotechnol 2003; 21: 519–25.
11. Bradley D W. Studies of non-A, non-B hepatitis and characterization of the hepatitis C virus in chimpanzees. Curr Top Microbiol Immunol 2000; 242: 1–23.
12. Weiss G, Umlauft F, Urbanek M, et al. Associations between cellular immune effector function, iron metabolism, and disease activity in patients with chronic hepatitis C virus infection. J Infect Dis 1999; 180: 1452–8.
13. Burgio V L, Ballardini G, Artini M, et al. Expression of co-stimulatory molecules by Kupffer cells in chronic hepatitis of hepatitis C virus etiology. Hepatology 1998; 27: 1600–6.
14. Castilla A, Prieto J, Fausto N. Transforming growth factors beta 1 and alpha in chronic liver disease. Effects of interferon alfa therapy. N Engl J Med 1991; 324: 933–40.
15. McCune J M, Namikawa R, Kaneshima H, et al. The SCID-hu mouse: murine model for the analysis of human hematolymphoid differentiation and function. Science 1988; 241: 1632–9.
16. Stoddart C A, Liegler T J, Mammano F, et al. Impaired replication of protease inhibitor-resistant HIV-1 in human thymus. Nat Med 2001; 7: 712–8.
17. Ilan E, Arazi J, Nussbaum O, et al. The hepatitis C virus (HCV)-Trimera mouse: a model for evaluation of agents against HCV. J Infect Dis 2002; 185: 153–61.
18. Shultz L D, Schweitzer P A, Christianson S W, et al. Multiple defects in innate and adaptive immunologic function in NOD/LtSz-scid mice. J Immunol 1995; 154: 180–91.
19. Yonou H, Yokose T, Kamijo T, et al. Establishment of a novel species- and tissue-specific metastasis model of human prostate cancer in humanized non-obese diabetic/severe combined immunodeficient mice engrafted with human adult lung and bone. Cancer Res 2001; 61: 2177–82.
20. Wernicke D, Schulze-Westhoff C, Brauer R, et al. Stimulation of collagenase 3 expression in synovial fibroblasts of patients with rheumatoid arthritis by contact with a three-dimensional collagen matrix or with normal cartilage when coimplanted in NOD/SCID mice. Arthritis Rheum 2002; 46: 64–74.
21. Ikeda M, Yi M, Li K, et al. Selectable subgenomic and genome-length dicistronic RNAs derived from an infectious molecular clone of the HCV-N strain of hepatitis C virus replicate efficiently in cultured Huh7 cells. J Virol 2002; 76: 2997–3006.
22. Takeuchi T, Katsume A, Tanaka T, et al. Real-time detection system for quantification of hepatitis C virus genome. Gastroenterology 1999; 116: 636–42.
23. Nuovo G J, Macconnell P, Forda A, et al. Detection of human papillomavirus DNA in formalin-fixed tissues by *in situ* hybridization after amplification by polymerase chain reaction. Am J Pathol 1991; 139: 847–54.
24. Nuovo M, Nuovo G. Utility of HHV8 RNA detection for differentiating Kaposi's sarcoma from its mimics. J Cutan Pathol 2001; 28: 248–55.